

Numerical simulation of the pre-ionization processes during nanosecond-pulse discharge in nitrogen

D. Levko,^{a)} V. Tz. Gurovich, and Ya. E. Krasik
Department of Physics, Technion, 32000 Haifa, Israel

(Received 4 October 2011; accepted 23 November 2011; published online 13 January 2012)

The pre-ionization of nitrogen gas by high-voltage nanosecond pulse discharges is studied using one-dimensional particle-in-cell numerical simulations. The comparison between the various mechanisms of pre-ionization, i.e., by runaway electrons, x-rays, and ultraviolet radiation, is presented. It is shown that runaway electrons produce a much higher number of electron-ion pairs than those generated by x-rays, which accompany the process of runaway electron generation. Also, results of simulations showed that among photo-ionization mechanisms the most significant gas pre-ionization is caused by x-rays generated in the process of impact ionization of the *K*-shell of nitrogen atoms. © 2012 American Institute of Physics. [doi:10.1063/1.3675439]

Nowadays, nanosecond time scale high-voltage (HV) gas discharges are used in various applications, for instance, x-ray generation, laser pumping, pressurized gap spark switches, and so on.¹ Such discharges are characterized by the velocity of the ionization front propagation, up to $\sim 10^9$ cm/s, which is explained²⁻⁵ by the pre-ionization of the discharge gap by runaway electrons (RAE). The latter are generated during the rise time of the discharge current in the vicinity of the cathode. The propagation of RAE across the cathode-anode (CA) gap leads to the generation of a dilute plasma, i.e., pre-ionization of the CA gap. Recent experiments⁶⁻¹¹ also showed that nanosecond discharges are accompanied by x-rays fluxes generated by RAE interaction with the anode and background gas atoms and molecules inside the CA gap. These x-rays fluxes can photo-ionize the gas and could affect the temporal and spatial evolution of the gas discharge.

The first experimental observation of photo-ionizing radiation formed by avalanching electrons was reported by Raether¹² in experiments of gas discharge supplied by a HV pulse with duration of $\sim 10^{-7}$ s. The experimental results showed a significant deviation from the theoretically predicted absorption coefficients, which makes these results questionable.¹³ Lozanskij and Firsov¹³ proposed a mechanism of photo-ionization based on the process $A^* + B \rightarrow AB^+ + e$, where A^* is the excited atom, B is the atom, AB^+ is the molecular ion, and e is the electron. However, this mechanism describes the discharge formation with a time scale of $\sim 10^{-7}$ s, and therefore it cannot be considered for the nanosecond time scale gas discharges.

There is another possible photo-ionization mechanism that is used to describe the gas discharge. This mechanism considers molecules C and D having different ionization potentials.¹⁴ Namely, if the ionization potential of molecule D is smaller than the excitation energy of molecule C , then the electron-ion pairs could be generated in the processes: $C + e \rightarrow C^* + e \rightarrow C + e + hv \rightarrow D + hv \rightarrow D^+ + e$. However, this mechanism cannot provide efficient pre-ionization of the

CA gap in nanosecond time as the typical spontaneous emission times of excited atoms and molecules exceed 10 ns.^{13,14} Also, this mechanism does not explain the high velocity of the ionization wave propagation. Indeed, in their report of experiments where the propagation of the cathode-directed streamer in the N_2 - O_2 mixture was studied, Starikovshii *et al.*¹⁵ stated that photo-ionization processes could provide an ionization front velocity of only $\sim 10^7$ cm/s.

Kozyrev *et al.*⁹ studied the sub-nanosecond discharge at atmospheric pressure and obtained that RAE generate the characteristic radiation of oxygen and nitrogen. It was suggested that this characteristic radiation efficiently generates secondary electrons and could be responsible for the formation of the diffusive instead of streamer-like discharge.

This paper presents the results of a comparison between different mechanisms of pre-ionization of the discharge gap filled with molecular nitrogen at atmospheric pressure during HV nanosecond discharge. It is shown that the pre-ionization of the gas by the photons having characteristic radiation is indeed the most efficient process among other photo-ionization mechanisms, although this mechanism is significantly less efficient than pre-ionization by RAE.

In order to study the processes accompanying the nanosecond discharge, one dimensional particle-in-cell (1D PIC) simulations were used.¹⁶ A coaxial diode filled with N_2 gas at 10^5 Pa pressure and with cathode and anode radii of $3 \mu\text{m}$ and 1 cm , respectively, and length of 1 cm was considered. Briefly, the sequence of 1D PIC simulation was as follows: (a) solution of the Poisson equation at the beginning of each time step for new electron and ion space charge densities and for new boundary conditions: zero anode potential and cathode potential varying in time as $\varphi_c = -\varphi_0 \sin(2\pi \cdot t/T)$, where $\varphi_0 = 120 \text{ kV}$ is the maximal cathode potential and $T/4 = 0.5 \text{ ns}$ is the rise time of the cathode potential; (b) calculation of the number of emitted electrons, which was defined by field emission (FE) governed by the Fowler-Nordheim (FN) law¹⁴; (c) study electron elastic and inelastic collisions¹⁷ (ionization, ionization of *K*-shell, bremsstrahlung, and excitation of the electron levels $A^3\Sigma_u^+$ and $C^3\Pi_u$) using the Monte-Carlo methods and, in addition, electron

^{a)}Author to whom correspondence should be addressed. Electronic mail: dlevko@physics.technion.ac.il.

scattering forward and backward was considered as well; and (d) particles weighting on the spatial grid and returning to step (a). The time step of 10^{-14} s allows us to consider electrons propagating only a part of the mean free path during one time step.

Figure 1(a) shows the time dependence of RAE numbers with the energies $\varepsilon_e \geq 1$ keV and $\varepsilon_e \geq 20$ keV propagating inside the CA gap. One can see that the generation of RAE with $\varepsilon_e \geq 20$ keV is terminated during the HV pulse rise time, whereas the insignificant generation of RAE with $\varepsilon_e \geq 1$ keV continues even when the cathode potential decreases. These data are explained by the formation of the virtual cathode (VC), which screens the FE of electrons and terminates the generation of RAE with $\varepsilon_e \geq 20$ keV in the vicinity of the cathode.¹⁶ The time of the VC formation at the considered conditions is $t_{VC} \approx 0.24$ ns. When the electric field at the VC location toward the anode exceeds 4.5×10^5 V/cm, the VC becomes the source of RAE. However, the electric field at VC is not sufficient to produce high-energy ($\varepsilon_e \geq 20$ keV) RAE and the majority of RAE obtain energy $20 \text{ keV} \geq \varepsilon_e \geq 1 \text{ keV}$ [see Fig. 1(c)]. In Fig. 1(c), the time $t \approx 0.5$ ns is selected because at that time the potential at the cathode reaches its maximal value. Figure 1(b) shows that the time evolution of the number of electron-ion pairs dN_{ei}/dt produced by the electrons with $\varepsilon_e \geq 1$ keV and $\varepsilon_e \geq 20$ keV per time step follows a time evolution of N_{RAE} .

In order to estimate the largest number of electronically excited N_2 molecules generated in the considered conditions, the additional channel of inelastic electron energy losses was considered in the simulations, namely, the excitation of the $N_2(C^3\Pi_u)$ [hereafter denoted as $N_2(C)$] energy level. The excitation cross-section of $N_2(C)$ is the largest among the excitation cross-sections of levels whose deexcitation results in ultraviolet radiation.¹⁷ In addition, the $N_2(C)$ excitation is an important component in N_2 gas discharge kinetic processes.¹⁴ It was shown that the radiation of $N_2(C)$ has the greatest intensity among the other species in sub-nanosecond discharges.⁹ Figure 1(c) shows the radial distribution of $N_2(C)$ inside the CA gap at $t \approx 0.5$ ns and the potential distribution at the same time. One can see that the largest number ($\sim 8 \times 10^9$) of $N_2(C)$ is excited inside the potential well (KOK*), where one obtains also the largest number of electrons with $\varepsilon_e \approx 11$ eV, i.e., with the energy of excitation of $N_2(C)$. However, simulation results showed that the largest

number of $N_2(C)$ generated per time step along the whole CA gap does not exceed $\approx 5 \times 10^5$, i.e., the electronically excited N_2 molecules cannot produce the number of UV-photons sufficient for gas pre-ionization at the considered time scale. Also, the UV-radiation of electronically excited ions N_2^+ cannot sufficiently pre-ionize the gas because of smaller excitation cross-sections of N_2^+ ions as compared with excitation cross sections of N_2 , and the lower density of N_2^+ than of N_2 molecules.¹⁴

Another possible source of ionizing radiation inside the CA gap is the radiation of electrons being accelerated in the extremely high electric field in the cathode's vicinity. The emitted energy in the frequency interval $d\omega/2\pi$ is determined by the Fourier component of the dipole moment,¹⁸ which is defined as $d = eat^2/2$. Here e is the electron charge, a is the electron's acceleration, and t is the time. Thus, the electromagnetic energy emitted in the frequency range $d\omega$ is

$$dE_\omega = \frac{16e^2 a^2 d\omega}{3c^3 \omega^2 2\pi}. \quad (1)$$

Here c is the light velocity. One can estimate the maximal value of the electric field considering one micro-protrusion on the cathode surface and its explosion. The current density of electrons emitted by this micro-protrusion can be estimated as $j^2 \approx h/t_d$, where $h = 1.4 \times 10^9 A^2 s/cm^4$ is the action integral of iron, and t_d is the delay time of this micro-protrusion explosion.¹ Assuming that the micro-protrusion emitting area is $\sim 6.3 \times 10^{-8} \text{ cm}^2$ and that the time delay is equal to the HV rise time of 0.5 ns, one obtains from the FN law that the electric field $E_{max} \approx 4.7 \times 10^7$ V/cm and the total number of emitted electrons during the delay time is $N_{max} \approx 3.3 \times 10^{11}$. To ionize N_2 molecules (ionization energy is ~ 16 eV), one requires photons with frequency $\omega_0 \geq 2.6 \cdot 10^{16} \text{ s}^{-1}$. Integrating Eq. (1) in the range (ω_0, ∞) one obtains that the maximum energy emitted during the acceleration of one electron is $\varepsilon_0 = 2 \cdot 10^{-28}$ J, and total energy emitted by the electrons is $N_{max} \varepsilon_0 \approx 6.6 \cdot 10^{-17} \text{ J} \approx 400 \text{ eV}$. Thus, one obtains that only ~ 25 photons with energy sufficient for ionization of N_2 molecules can be emitted by this process. Now, supposing that there are up to 10^4 micro-protrusions,¹ one obtains a total number of high energy photons of $\sim 2.5 \times 10^5$. Even if all of these photons ionize molecules, the number of generated electron-ion pairs will still be significantly smaller than the

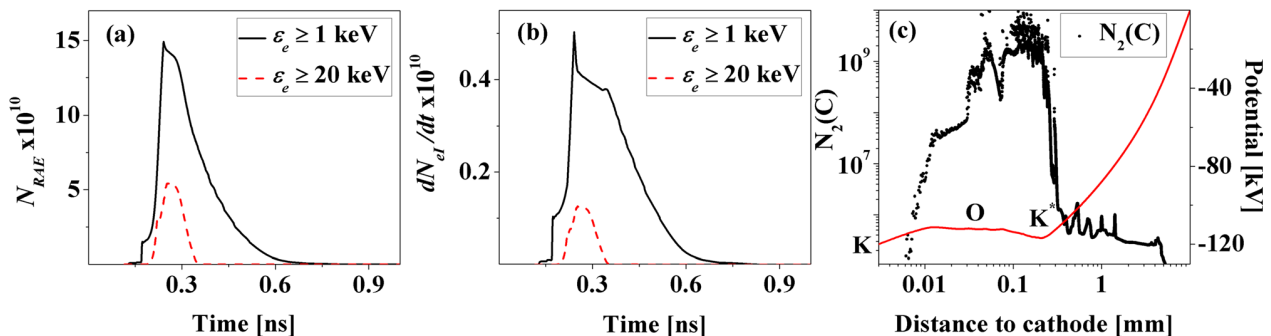


FIG. 1. (Color online) (a) Time dependence of the total RAE number inside the CA gap with energies ≥ 1 and ≥ 20 keV; (b) time dependence of electron-ion pairs generated per time step by RAE with energies ≥ 1 and ≥ 20 keV; and (c) space distribution of the potential and $N_2(C)$ number at $t \approx 0.5$ ns.

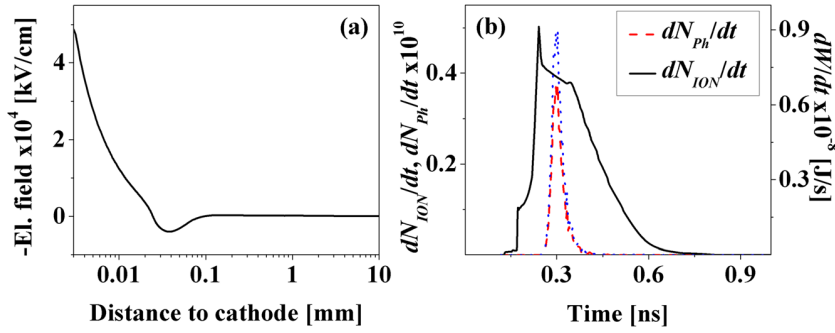


FIG. 2. (Color online) (a) Electric field distribution in the CA gap at $t \approx 0.23$ ns; (b) time dependence of the numbers of x-rays emitted from the anode and electron-ion pairs generated per time step inside the CA gap by RAE with $\varepsilon_e \geq 1$ keV; time dependence of the energy emitted by x-rays from the anode (blue dotted line).

number of secondary electrons produced in inelastic collisions by RAE and N_2 molecules. Let us note also that the electric field is not uniform inside the CA gap. Figure 2(a) shows the electric field distribution in the CA gap at $t \approx 0.23$ ns, i.e., immediately before the VC formation. At this time the electric field at the cathode almost reaches its maximum value. One can see that E already decreases by an order of magnitude at a distance of ~ 0.01 mm with respect to the cathode. This leads to a decrease by 2 orders of magnitude in the number of photons that could ionize neutrals.

High energy x-rays are also produced when RAE penetrate the anode. A total x-ray energy per unit time produced in the anode by RAE with energies ε_e can be estimated following Kremnev and Kurbatov⁵:

$$dW = kZe^2 \cdot (eN_{RAE}/dt) \times \exp(-\mu(\lambda) \times \delta). \quad (2)$$

Here δ is the anode thickness, $k = 10^{-3} \text{ V}^{-1}$, Z is the atomic charge of the anode material, eN_{RAE}/dt is the current of RAE with energy ε_e entering the anode, and $\mu(\lambda)$ is the absorption coefficient for x-rays with wavelength λ .¹⁹ In the model, the anode considered was made of aluminum foil with a thickness of $\delta = 12.5 \mu\text{m}$. Figure 2(b) shows the comparison between the numbers of photons emitted from the anode and electron-ion pairs generated in the CA gap by electrons with $\varepsilon_e \geq 1$ keV per time step and the energy of x-rays emitted from the anode per time step. Here, the number of photons was estimated as the energy calculated from Eq. (2) divided by the ionization energy of N_2 and by a factor of 2, which takes into account that only a half of the generated photons are emitted into the CA gap. One can see [Fig. 2(b)] that the

maxima of the electron-ion pair and photon numbers are shifted in time. The first maximum appears when the number of RAE with $\varepsilon_e \geq 1$ keV reaches the maximum value, which coincides with the time of VC formation. The space distributions of the electrons with $\varepsilon_e \geq 1$ keV at $t = t_{VC} \approx 0.24$ ns and at $t \approx 0.32$ ns are shown in Figs. 3(b) and 3(c). One can see that the VC terminates the generation of electrons with $\varepsilon_e \geq 1$ keV. In Figs. 3(b) and 3(c) the times $t \approx 0.24$ ns and $t \approx 0.32$ ns were selected to show the space distribution of electrons with the $\varepsilon_e > 1$ keV at times when the VC is formed and after its formation. The maximum of number of photons appears when one obtains the largest RAE flow at the anode during one time step. Nevertheless, the number of photons emitted from the anode is significantly smaller than the number of electron-ion pairs generated by RAE. Thus, the x-ray photons generated by RAE interaction with the anode cannot pre-ionize the gas more efficiently than the RAE.

Kozyrev *et al.*⁹ proposed gas pre-ionization in the CA gap by soft x-rays generated by RAE bremsstrahlung radiation on the nuclei of atoms and K -shell impact ionization of atoms, which results in characteristic radiation. The total cross-section of bremsstrahlung radiation is⁹:

$$\sigma_\omega \approx \frac{8e^2}{3hc^3} \left(\frac{Ze^2}{mv_0} \right)^2 \ln^2 \left(\frac{2mv_0^2}{\gamma \cdot Ze^2 \omega_{\min}} \right), \quad (3)$$

where m is the electron mass, $Z=7$ for N atoms, v_0 is the electron's velocity, $\gamma \approx 1.781$ is the relativistic factor, and $\hbar\omega_{\min} = 300$ eV. The characteristic radiation cross-section is defined as⁹

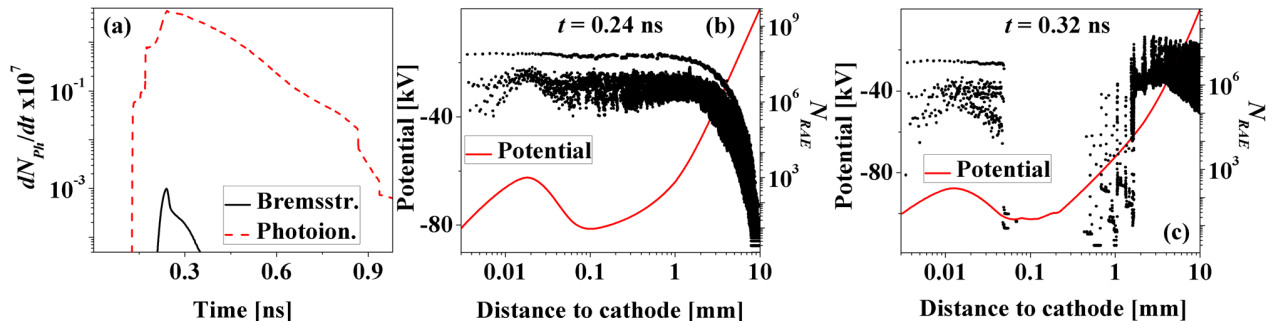


FIG. 3. (Color online) (a) Time dependence of bremsstrahlung and photo-ionization photons; (b,c) Space distribution of potential and number of electrons with $\varepsilon_e \geq 1$ keV at $t \approx 0.24$ ns and $t \approx 0.32$ ns, respectively.

$$\sigma_z(\varepsilon) \approx \frac{10^{-24} \text{cm}^2}{I_z \varepsilon (\varepsilon + 2)} \left\{ 2 + (\varepsilon + 1)^2 \ln \sqrt{\frac{\varepsilon(\varepsilon + 1)}{I_z}} - \frac{I_z}{\varepsilon} \left[(\varepsilon + 2)^2 + 2(2\varepsilon + 1) \ln \frac{\varepsilon}{I_z} - 2 \right] \right\}. \quad (4)$$

Here $I_z = \varepsilon_z/mc^2$, $\varepsilon = mv_0^2/2mc^2$, and $\varepsilon_z \approx 405$ eV is the ionization energy of K -shell of N atom.⁹

Figure 3(a) shows the comparison between the numbers of bremsstrahlung and characteristic photons produced per time step. One can see that the number of photon characteristics exceeds $\sim 10^2$ times the number of bremsstrahlung photons because of the bremsstrahlung cross-section (3) being smaller than the cross section of characteristic radiation (4). Thus, gas pre-ionization by the bremsstrahlung photons can be considered negligibly small as compared with gas pre-ionization by characteristic photons and RAE. The largest number of characteristic photons is produced prior to the VC formation by inelastic $e - N_2$ collisions for electrons with $\varepsilon_e > 10$ keV, which are obtained at a distance $r > 10 \mu\text{m}$ with respect to the cathode. As the VC generates a much smaller number of RAE with $\varepsilon_e > 10$ keV than in the vicinity of the cathode, the number of characteristic photons decreases significantly after the VC formation. Nevertheless, the comparison between the numbers of characteristic photons and of electron-ion pairs produced by the electrons with $\varepsilon_e \geq 1$ keV shows that the pre-ionization by RAE is much more efficient [see Figs. 3(a) and 3(b)].

To conclude, the results of the numerical simulation of N_2 gas pre-ionization in HV nanosecond pulse discharge by RAE and x-rays showed that the number of electron-ion pairs generated by RAE is significantly larger than of those generated by x-rays. The probability for electrons to be scattered at large angles by collisions is small,¹⁴ and, therefore, the RAE pre-ionize the gas in a narrow range of angles. At the same time, the results of numerical simulation, where energy spectrum of energetic electrons was used, confirmed

analytical evaluation⁹ that the most intensive soft x-ray generation occurs in the process of K -ionization of N atoms. The characteristic photons are emitted uniformly in all directions and therefore pre-ionize the whole volume of the CA gap leading to the diffuse discharge formation.⁹

ACKNOWLEDGMENTS

This work was supported in part at the Technion by a fellowship from the Lady Davis Foundation.

- ¹G. A. Mesyats, *Pulsed Power and Electronics* (Nauka, Moscow, 2004) (in Russian).
- ²L. P. Babich, T. V. Loiko, and V. A. Tsukerman, *Phys. Usp.* **33**, 521 (1990).
- ³G. A. Mesyats, M. I. Yalandin, K. A. Sharypov, V. G. Shpak, and S. A. Shunailov, *IEEE Trans. Plasma Sci.* **36**, 2497 (2008).
- ⁴V. F. Tarasenko and S. I. Yakovlenko, *Phys. Usp.* **47**, 887 (2004), and references therein.
- ⁵L. P. Babich, *High-Energy Phenomena in Electric Discharges, Vol. 2* (Futurepast, Arlington, Virginia, 2003).
- ⁶A. G. Rep'ev and P. B. Repin, *Techn. Phys.* **53**, 73 (2008), and references therein.
- ⁷L. P. Babich and T. V. Loiko, *Plasma Phys. Rep.* **36**, 263 (2010).
- ⁸I. D. Kostyrya and V. F. Tarasenko, *Techn. Phys.* **55**, 270 (2010), and references therein.
- ⁹A. V. Kozyrev, V. F. Tarasenko, E. Kh. Baksht, and Yu. V. Shut'ko, *Techn. Phys. Lett.* **37**, 1054 (2011).
- ¹⁰Tao Shao, Cheng Zhang, Zheng Niu, Ping Yan, V. F. Tarasenko, E. Kh. Baksht, I. D. Kostyrya, and V. Shutko, *J. Appl. Phys.* **109**, 083306 (2011).
- ¹¹T. Shao, C. Zhang, Z. Niu, P. Yan, V. F. Tarasenko, E. Kh. Baksht, A. G. Burachenko, and Yu. V. Shutko, *Appl. Phys. Letters* **98**, 021503 (2011).
- ¹²H. Raether, *Z. Phys.* **110**, 611 (1938).
- ¹³E. D. Lozanskij and O. B. Firsov, *The Theory of Spark* (Atomizdat, Moscow, 1975) (in Russian).
- ¹⁴Yu. P. Raizer, *Gas Discharge Physics* (Springer, Berlin, 1991).
- ¹⁵S. V. Pancheshnyi, S. M. Starikovskaya, and A. Yu. Starikovskii, *J. Phys. D: Appl. Phys.* **34**, 1 (2001).
- ¹⁶D. Levko, S. Yatom, V. Vekselman, J. Z. Gleizer, V. Tz. Gurovich, and Ya. E. Krasik, "Numerical simulations of runaway electrons generation in pressurized gases," *J. Appl. Phys.* (to be published).
- ¹⁷Y. Itikawa, *J. Phys. Chem. Ref. Data* **35**, 31 (2006).
- ¹⁸L. D. Landau, *Field Theory* (Nauka, Moscow, 1988) (in Russian).
- ¹⁹NIST: <http://physics.nist.gov/PhysRefData/XrayMassCoef/tab3.html>.